M&C 2017 - International Conference on Mathematics & Computational Methods Applied to Nuclear Science & Engineering, Jeju, Korea, April 16-20, 2017, on USB (2017)

Re-evaluation of the ^{154}Eu thermal capture cross-section based on spent fuel benchmarking studies

Steven E. Skutnik

Department of Nuclear Engineering, University of Tennessee-Knoxville, 1508 Estabrook Road, Knoxville, TN 37996
sskutnik@utk.edu

Abstract - *^{154}Eu is an important burnup indicator nuclide, especially for assays of longer-cooled fuel assemblies, given its comparatively longer half-life of 8.593 years and its high-energy gamma emissions. However, recent integral benchmarking studies based on spent fuel assay data reveals evidence of a systematic bias in the thermal-region $^{154}Eu\,(n,\gamma)\,^{155}Eu$ capture cross-section, wherein evaluations within the ENDF/B-VII.0 and VII.1 libraries underestimate the radiative capture cross-section in this region. As a result, ^{154}Eu is consistently overestimated in spent fuel benchmarking studies. In this study, a corrected evaluation of the ^{154}Eu capture cross-section is presented, which is benchmarked across 14 spent fuel assay benchmarks. In general, the new proposed evaluation shows about 5–6% better agreement with experimental data than the ENDF/B-VII.0 and VII.1 evaluations for light water reactor data and an even greater improvement for the pressurized heavy water reactor benchmark studied.*

I. INTRODUCTION

^{154}Eu is an important burnup indicator nuclide, given its relatively energetic gamma emissions (996.3 keV, 1,004.8 keV, and 1,274.4 keV) and moderately long half-life (8.59 years). In as much, ^{154}Eu is frequently used in conjunction with ^{137}Cs) as a passive indicator of spent fuel burnup [1], especially for longer-aged assemblies (i.e., cooled for > 5000 days). The ^{154}Eu signature is therefore important to a number of applications, including measurements used for spent fuel burnup credit [2] and for fuel assembly burnup estimation for safeguards applications (including reconstruction of plutonium content of irradiated assemblies) [3, 4].

However, a number of recent benchmarking studies employing the most recent ENDF nuclear data evaluations (ENDF/B-VII.0 and VII.1) have uncovered evidence of systematic overestimation in the predicted inventories of ^{154}Eu across a diverse set of assembly types, as evinced in Table I. ^{154}Eu is consistently over-predicted in spent fuel benchmark studies, generally on the order of 10% or more; this stands in marked contrast with relatively accurate calculations of both actinoid inventories as well as other major burnup indicator species, such as ^{137}Cs and ^{148}Nd. Thus, in this paper I present evidence of a systematic bias in calculated spent fuel isotopic inventories arising from underestimation of the thermal capture cross-section for the $^{154}\mathrm{Eu\,(n,\gamma)\,}^{155}$Eu reaction in the most recent ENDF evaluations.

This study is based off of benchmarking studies from several well-documented spent fuel destructive assay benchmarks covering a range of fuel burnups and assembly types, including a CANDU pressurized heavy water reactor (PHWR) assembly as well as a number of different pressurized water reactor (PWR) fuel assembly lattice types. The findings of this study indicate that the overestimation effect arising from the thermal radiative capture cross-section is both persistent as well as sensitive to spectral effects (i.e., the effect is most pronounced in more heavily moderated spectra with a lower average neutron energy, such as in the CANDU PHWR assembly).

II. BACKGROUND & THEORY

1. ^{154}Eu production and destruction

Because the direct fission yield of ^{154}Eu from both ^{235}U and ^{239}Pu fission is vanishingly small and production of ^{154}Eu from beta decay is blocked by the stable isotope ^{154}Eu, the dominant production channel for ^{154}Eu is through neutron capture reactions; i.e., ^{154}Eu is produced almost exclusively from neutron captures by ^{153}Eu. As a result, ^{154}Eu are proportional to neutron exposure, similar to ^{134}Cs, another commonly-employed burnup indicator species. Meanwhile, given the long half-life of ^{154}Eu, the dominant loss mechanism during irradiation is through successive radiative capture by ^{154}Eu (producing ^{155}Eu).

In as much, over-estimation of the ^{154}Eu inventories can be narrowed down to one of two causes: over-production of ^{154}Eu (either directly by over-estimation of the rate of neutron captures by ^{153}Eu or over-production of ^{153}Eu directly from fission), or from under-estimation of losses of ^{154}Eu from capture reactions. In the case of over-estimations of ^{153}Eu driving over-predictions of ^{154}Eu (either due to overestimation of ^{153}Eu production or capture losses), one should expect to see a correlated pattern of systematic overestimations of ^{153}Eu inventories. Conversely, a relatively good agreement of ^{153}Eu predictions with benchmark data would imply an issue with the ^{154}Eu loss channel. As I will illustrate in the following section, evidence strongly points to this latter explanation.

2. ^{153}Eu & ^{154}Eu radiative capture cross-section evaluations

Figures 1 and 2 illustrate the radiative capture cross-sections for ^{153}Eu and ^{154}Eu across different nuclear data evaluations. With the exception of the transition from ENDF/B-VII.0 to VII.1 (wherein there is a 15% upward adjustment in the $^{153}\mathrm{Eu\,(n,\gamma)\,}^{154}$Eu thermal capture cross-section due to new experimental data incorporated into the evaluation), the ^{153}Eu radiative capture cross-section is effectively unchanged between evaluations. Thus, while enhanced capture by ^{153}Eu in the ENDF/B-VII.1 evaluation would explain a small com-

TABLE I. Calculated to experiment (C/E) ratios for ^{154}Eu from recent spent fuel benchmarking studies using ENDF/B-VII.0 and VII.1 data; ENDF/B-VII.0 and VII.1 C/E data adapted from evaluations in [5] with original benchmarking studies indicated.

Assembly / Sample	Type	# samples	$\overline{\sigma}$	Average C/E	
				ENDF-VII.0	ENDF-VII.1
TMI-1 NJ05YU [6]	B&W 15 × 15 (PWR)	5	0.021	1.1151	1.1311
Calvert Cliffs MKP-109 [7]	CE 14 × 14 (PWR)	3	0.074	1.0647	1.0924
REBUS GKN-II [8]	18 × 18 (PWR)	1	0.017	1.1320	1.1448
ARIANE GU1 [8]	15 × 15 (PWR)	1	0.020	1.1283	1.1391
Vandellós II [9]	Westinghouse 17 × 17 (PWR)	3	0.104	1.0971	1.1209
Pickering-A 19558C [10]	CANDU 28-element (PHWR)	1	0.050	1.1623	1.2641

ponent of overestimates of ^{154}Eu, this alone is insufficient to explain the observed bias.

Meanwhile, one will observe that between the ENDF/B-VI.8 and VII.0 evaluations, there is a far more dramatic change to the thermal-region capture cross-section, wherein the thermal capture cross-section in ENDF/B-VI.8 (evaluated by R.Q. Wright of ORNL) of 1840 barns is based on measurements conducted by Sekine et. al. [11]; ENDF/B-VII.0 reports a value of 1340 ± 130 barns calculated by Mughabghab [12], a 36.6% difference. This significant change in the absorption cross-section would easily explain the overestimations in the ^{154}Eu inventories observed, namely by suppressing the thermal capture rate by ^{154}Eu.

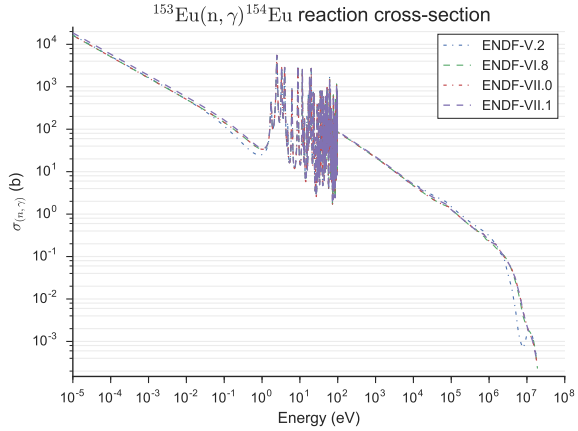

Fig. 1. ^{153}Eu (n, γ) ^{154}Eu capture cross-section for ENDF/B-V.2, VI.8, VII.0, and VII.1 evaluations [13, 14]. Note that the ENDF/B-VII.1 evaluation shows a 15% change in the thermal capture cross-section based upon new measurements included in the evaluation.

Mughabghab points out that the 1840 barn thermal capture cross-section reported by Sekine et. al. assumes a $^1/_v$ Wescott factor of unity, wheras the correct value would be g_w = 1.237 [5]; thus, the true thermal capture cross-section (rather than the Maxwellian-weighted value) would be around 1488 ± 73 barns [5]. For comparison, historical evaluated values of the 2200 $^m/_s$ cross-section are reported in Table II; here, one will observe that the corrected Sekine value lies just over the 1-σ uncertainty bounds from the original value reported by

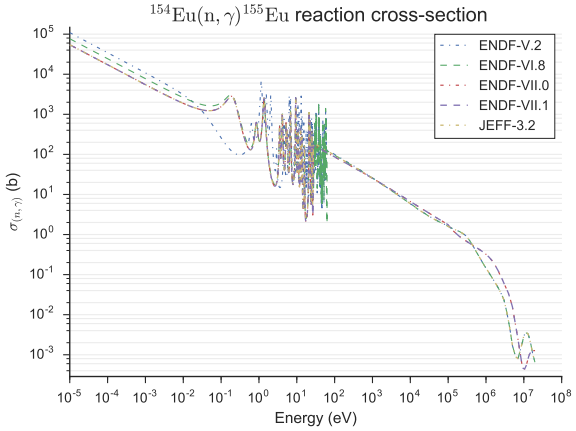

Fig. 2. ^{154}Eu (n, γ) ^{155}Eu capture cross-section for ENDF/B-V.2, VI.8, VII.0, and VII.1 evaluations. [13, 14]. The ^{154}Eu thermal capture cross-section (below 0.1 eV) is approximately 37% lower in ENDF/B-VII.0 and VII.1 evaluations as compared to ENDF/B-VI.8.

Mughabghab [12]. This Wescott-corrected value will serve as a basis of comparison for proposed revisions to the cross-section value discussed in the next section.

TABLE II. Measured and evaluated 2200 $^m/_s$ capture cross-sections (σ_{th}) for ^{154}Eu

Evaluator	Type	σ_{th} (bn)	Uncert. (bn)
Hayden et. al. [15]	Exp.	880	—
Vertebnyj et. al. [16]	Exp.	1250	160
Sekine et. al. [11]	Exp.	1840	90
Mughabghab [12]	Calc.	1340	130

3. Evaluated modifications to the ^{154}Eu radiative capture cross-section

Based on the differences in the ENDF/B-VI.8 evaluation (performed by R. Q. Wright) and ENDF/B-VII.0, one amendment to the ^{154}Eu thermal capture cross-section that could be inferred would be to restore the resolved resonance treatments evaluated by Wright, including a bound state at -0.71 eV and adjusting the first resolved resonance at 0.190 eV (hereafter

referred to as the "Wright" evaluation). An alternative evaluation, proposed by Mughabghab, would be to shift the location of the first resolved resonance from 0.195 eV to 0.188 eV based on results reported by Anufriev [17]; this in turn would also incorporate adjusting the neutron width (Γ_n) proportional to $\frac{1}{\sqrt{E}}$, i.e. by a factor of $\sqrt{\frac{0.195}{0.188}} = 1.018$ (referred to hereafter as "Mughabghab"). The modifications ot the ENDF resolved resonance evaluations for each of these evaluations is explicitly shown as Table III.

Applying each of the two proposed modifications in Table III to the ENDF/B-VII.0 and VII.1 resolved resonances for ^{154}Eu, I developed new AMPX master continuous energy (CE) libraries for use with the TRITON/NEWT discrete ordinates transport sequence to evaluate the effect of modifying the thermal capture resolved resonance parameters. While TRITON/NEWT makes use of multi-group nuclear data in its lattice physics treatment, the CENTRM module used to process resonance self-shielding uses AMPX CE data to update the multigroup libraries; thus, updating the AMPX CE data used by TRITON was required to perform this evaluation. This updated CE data is then propagated by CENTRM into the calculation to produce updated multi-group libraries used in the lattice physics calculation.

The updated pointwise cross-sections for the thermal resonance region are shown in Figure 3. Here, the primary difference between the evaluations is in the centroid and intensity of the first resolved resonance and likewise the $^1/_v$ thermal region of the cross-section.

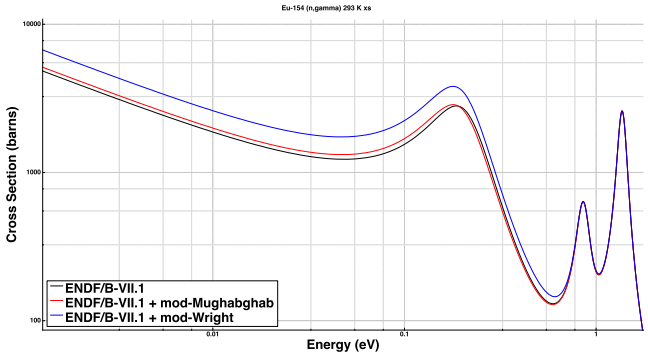

Fig. 3. Original ENDF/B-VII.0 & VII.1 treatment for the thermal region of the ^{154}Eu (n,γ) ^{155}Eu cross-section, along treatments based on restoring the ENDF/B-VI.8 bound state and first resolved resonance ("Wright") and by shifting the location of the first resolved resonance and adjusting the neutron width proportionally ("Mughabghab").

Note that previously-conducted integral benchmark evaluations using the Wright treatment appear to overestimate ^{154}Eu captures, leading to underestimation of the ^{154}Eu inventory in most samples evaluated [5]. Conversely, the Mughabghab treatment shows consistently improved agreement with experimental values for both ENDF/B-VII.0 and VII.1 although still producing noticable overestimates of ^{154}Eu inventories for most cases [5]. As a result, this analysis will focus exclusively upon the modifications to the ^{154}Eu thermal capture evaluation proposed by Mughabghab.

4. Integral benchmarks evaluated

For this study, fourteen samples from six separate assemblies are evaluated, spanning a range of burnups from 27.35–64.6 $\frac{\text{GWd}}{\text{MTU}}$ for PWR assembly types, along with one CANDU 28-element PHWR assembly with a discharge burnup of 9.21 $\frac{\text{GWd}}{\text{MTU}}$. Details of each set of benchmark evaluations are described in the following subsections.

A. TMI-1 NJ05YU samples

Five benchmark samples were obtained from Three-Mile Island Unit 1 (TMI-1) NJ05YU from two separate pins: samples C2D1 and C2D2 taken from pin H6 (an interior pin), and samples A1, B1, and B2 taken from pin D5, located next to a control rod guide tube, corresponding to the samples studied in [6], as illustrated Figure 4. For the first irradiation cycle (Cycle 9), sixteen Al_4-B_4C control rods were present in the guide tubes; these were removed in the second irradiation cycle (Cycle 10). This removal was modeled using TRITON's material swap feature (new to SCALE 6.2), with the control rod material swapped for an equivalent volume of moderator.

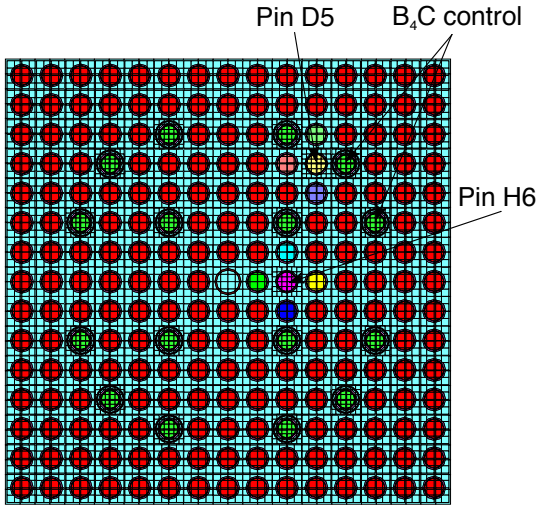

Fig. 4. TRITON lattice model for the TMI-NJ05YU samples evaluated (from pins D5 and H6, as indicated on the figure). B_4C control rods were removed (using TRITON's `swap` feature) following the first irradiation cycle.

B. Calvert Cliffs MKP-109 samples

Calvert Cliffs assembly D047 was a Combustion Engineering 14 × 14 (CE 14 × 14) PWR assembly measured as part of a U.S. campaign designed to measure moderate-burnup assemblies representative of many assemblies currently kept in on-site storage [7]. The Calvert Cliffs measurements consisted of three samples taken from rod MKP-109, an interior rod (illustrated in Figure 5), covering a sample burnup range of 27.4 $\frac{\text{GWd}}{\text{MTU}}$ to 44.3 $\frac{\text{GWd}}{\text{MTU}}$. As seen in Figure 7, assembly D047 is modeled as a half-lattice model with reflective boundary conditions owing to symmetry; the TRITON lattice model was constructed based on sample inputs provided in [7].

TABLE III. Evaluated modifications to the ENDF/VII.0 / VII.1 ^{154}Eu (n, γ)^{155} Eu resolved resonance parameters, based on the ENDF/B-VI.8 thermal-region behavior ("Wright") and changes proposed by Mughabghab ("Mughabghab"). Note that the changes based on ENDF/B-VI.8 ("Wright") introduces an additional bound state at -0.71 eV not present in the VII.0 or VII.1 evaluations.

Evaluation	E (eV)	$\|J\|$	Γ	Γ_n	Γ_γ
Wright	-0.7100000	2.5	0.1264160	4.160000E-4	0.1260000
	0.1900000	3.5	0.1600595	5.950000E-5	0.1600000
Mughabghab	0.1880000	2.5	0.1500731	7.307365E-5	0.1500000

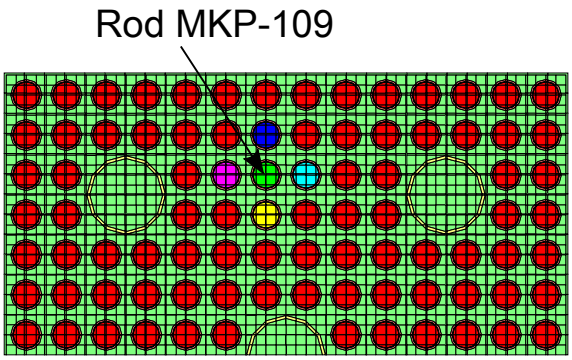

Fig. 5. TRITON half-assembly lattice model for the Calvert Cliffs rod MKP-109 samples evaluated.

Assembly D047 was irradiated over the course of four cycles, although simplifying the analysis, there were no burnable poisons or gadolinia (Gd_2O_3-UO_2) rods in the assembly. The cycle powers used to produce the benchmark evaluation were corrected from their nominal values published in [7, 18, 19] to match inventories of ^{148}Nd [5], used as strong indicator of the total number of fissions (and therefore actual fuel burnup) [20].

C. REBUS GKN-II sample

The REBUS program. comprised of an international collaboration of institutes from Belgium, France, Germany, Japan, and the United States, focused on code validation measurements used for burnup credit in spent fuel storage applications, employing critical experiments conducted on spent fuel rod segments [8]. Of these, rod M11 from assembly 419 of the Gemeinschaftskernkraftwerk Unit II (GKN-II) reactor in Germany (an 18×18 PWR assembly employing UO_2 fuel) was measured for its isotopic content. Key characteristics of this assembly include the presence of 12 gadlonia rods with 7.0 wt. % Gd_2O_3 content (with an initial uranium enrichment of 2.6 wt. %) and 24 guide tubes [8]. The measured rod (M11) was located relatively toward the interior of the assembly, away from flux-distorting features such as gadlonia rods and guide tubes (as seen in Figure 7), rendering the benchmark relatively free of possible biases that may confound isotopic comparisons.

D. ARIANE GU1 sample

The ARIANE program represented an international collaborative effort (coordinated by Belgonucleaire and involving

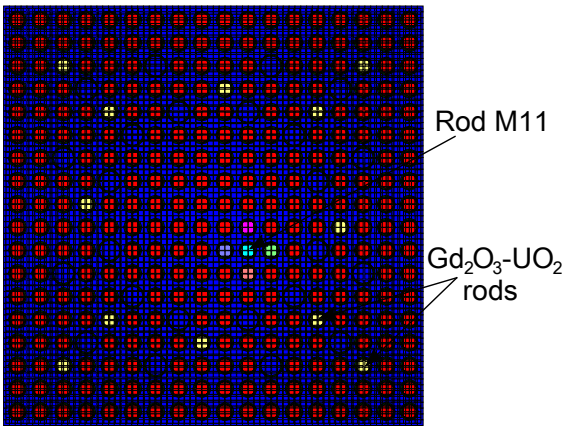

Fig. 6. TRITON lattice model for the REBUS GKN-II sample (from rod M11) evaluated. Note the presence of gadolinia burnable absorber (Gd_2O_3-UO_2) rods present in the assembly.

participant laboratories and utilities from Belgium, Germany, Japan, Netherlands, Switzerland, the U.K., and the U.S.) intended to expand available isotopic measurements from spent fuel assemblies used for validation of reactor physics and depletion codes [8]. Three UO_2 samples were measured by the ARIANE program (samples GU1, GU3, and GU4) from the Gösgen reactor located in Switzerland. However, due to substantial irregularities in the irradiation histories of samples GU3 and GU4, these samples were not considered for this study. GU3 and GU4 were irradiated within assembly 1601 for cycles 16 and 17 and subsequently transferred to a assembly 1701, which began cycle 18 with an average burnup of about 20.0 $\frac{\text{GWd}}{\text{MTU}}$ [8]. It was determined that the complexity of this operating history introduced the potential for significant confounding factors which may render benchmarks from these samples less useful for establishing the accuracy of the ^{154}Eu inventories, especially compared to less complex irradiation histories.

E. Vandellós-II samples

Three samples were evaluated from the Vandellós-II reactor from Spain as part of a program to evaluate especially high-burnup fuel samples [9]. This analysis focuses on three samples taken at different axial locations (samples E58-088, E58-148, and E58-263) from rod WZR0058, taken from assembly EC45. Rod WZR0058 was part of a Westinghouse 17×17 assembly; this rod was irradiated as part of assembly

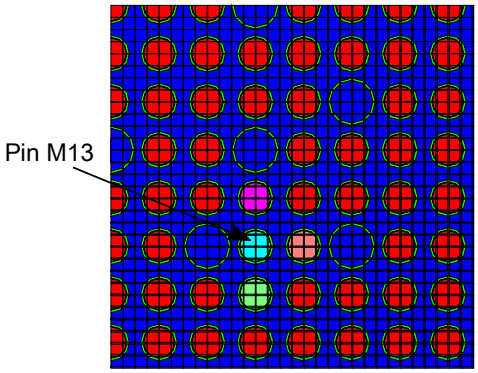

Fig. 7. TRITON quarter-assembly lattice model for the ARIANE GU1 assembly sample evaluated.

EC45 for three consecutive cycles (cycles 7–10) before being removed and placed into the rebuilt assembly EF05, which had a previous assembly-average burnup of 26.5 $\frac{\text{GWd}}{\text{MTU}}$ [9]. Three other samples were available in this benchmark (including sample E58-700 from WZR0058, sample 165-2a from rod WZtR165, and sample 160-800 from rod WZtR160), however these samples were not evaluated as part of this study due to inconsistencies in the calculated isotopic inventories (including major actinides and burnup indicator species like ^{148}Nd), potentially due to problems with the assay measurements themselves [9]. The TRITON lattice models used for modeling rod WZR0058 in cycles 7–10 and cycle 11 are presented as Figure 8 and 9, respectively.

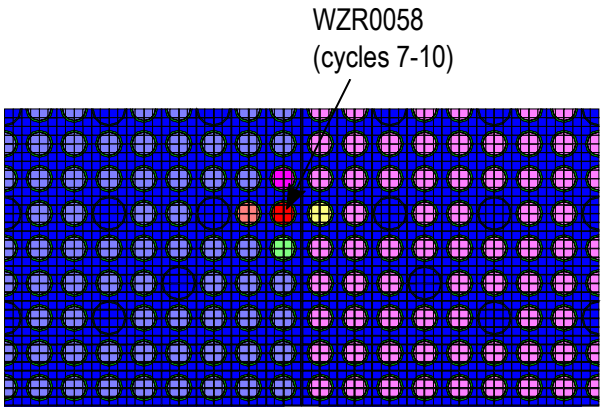

Fig. 8. TRITON lattice model for the Vandellós-II WZR0058 pin, cycles 7-10. Per [9], the neighboring quarter assembly was also modeled for cycles 7-10 in order to capture neighbor assembly effects, due to the location of pin WZR0058 at the edge of the assembly. Likewise note that pin WZR0058 was subsequently removed and placed into the rebuilt assembly EF05 for cycle 11.

Despite the overall complexity of the Vandellós irradiation history (similar to samples GU3 and GU4 of the ARIANE assembly which were not modeled), a reasonable agreement was obtained for major isotopes of both uranium and plutonium as well as burnup indicators such as ^{148}Nd and ^{137}Cs, with agreements within 2% for ^{148}Nd and well within the 2-σ

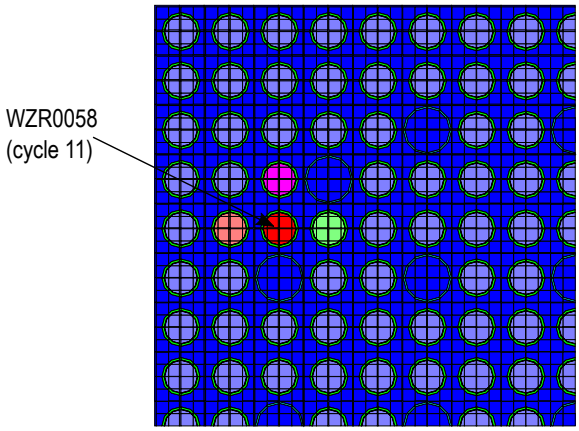

Fig. 9. TRITON quarter-assembly lattice model for the rebuilt Vandellós-II EF05 assembly for the WZR0058 pin, irradiated in cycle 11.

confidence bounds defined for the uranium and plutonium measurements [9], indicating a good overall agreement of the model ot the experimental assay.

F. Pickering-A 19558C / CANDU-28 element sample

Fuel bundle 19958C (irradiated in the Pickering-A reactor) is a 28-element CANDU PHWR assembly employing natural uranium fuel elements with Zircaloy-4 cladding, employing a heavy-water (D_2O) moderator, with the fuel lattice depicted as Figure 10, using a nominal assembly power history provided in [21]. Each ring of the assembly was modeled as a separate fuel material with a uniquely-calculated Dancoff Factor in order to accurately represent the differences in the neutron flux and element powers for each ring (given the unique geometry of CANDU fuel bundles); details of this model are provided in [10].

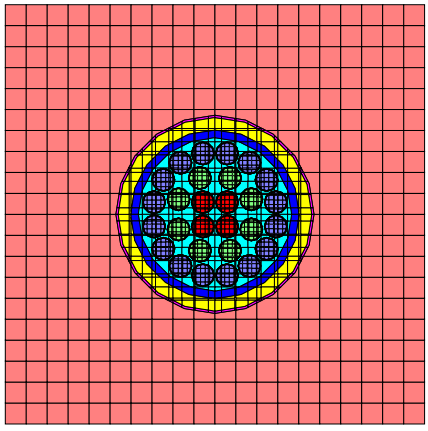

Fig. 10. TRITON assembly lattice model for the Pickering-A (bundle 19958C) CANDU 28-element PHWR bundle evaluated.

In the destructive chemical assay benchmark outlined in [21, 22, 23], a single outer-ring fuel element was assayed

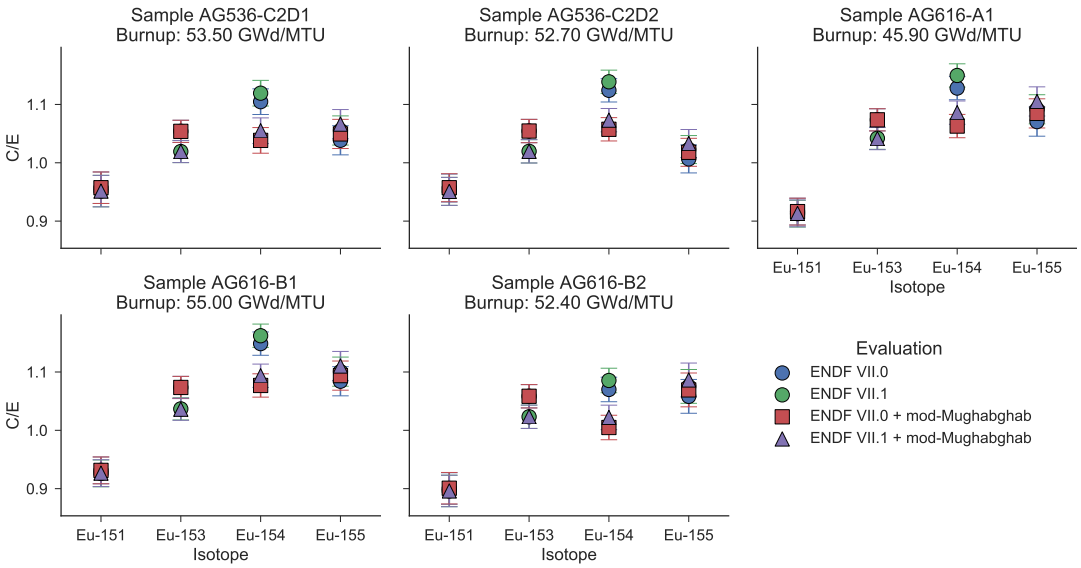

Fig. 11. C/E values for ^{151}Eu, ^{153}Eu, ^{154}Eu, and ^{155}Eu for the TMI-1 assembly NJ05YU benchmark for each nuclear data evaluation considered.

to provide benchmarking data for lattice physics depletion studies. The lattice used for the purposes of this depletion study is the same as that as evaluated in [10]; thus, for a more extended discussion of this validation effort, including modeling details, the reader is directed to this paper.

III. RESULTS AND ANALYSIS

1. Evaluation of Eu isotopes for individual spent fuel benchmarks

Figures 11–16 illustrate the difference between calculated and experimentally measured isotopes of europium for each of the benchmarks considered. For each benchmark, this difference is expressed as the ratio of calculated-to-expected (C/E).

For the TMI-1 NJ05YU samples (Figure 11), one observes a consistent and substantial increased agreement with the experimental benchmark for ^{154}Eu with the thermal-region modification for both ENDF/B-VII.0 and VII.1, wherein calculated ^{154}Eu inventories drop by approximately 6.5% following the thermal-region correction for both ENDF/B-VII.0 and VII.1 (as seen in Table IV, with an average C/E of approximately 5–6% for the corrected evaluations, which while still outside of the 2-σ confidence bounds is a significant improvement. One will note the slight increase in C/E values for ^{154}Eu when moving from the ENDF/B-VII.0 to the VII.1 evaluation, explainable from the increase in the ^{153}Eu capture cross-section within the VII.1 evaluation. Similarly, as observed in Figure 11, corrections to the bias in the ^{154}Eu produce a slight increase in the over-prediction of the ^{155}Eu inventory, an effect which is consistently observed across most of the other samples evaluated; this is attributable to the increased capture by ^{154}Eu, producing more ^{155}Eu.

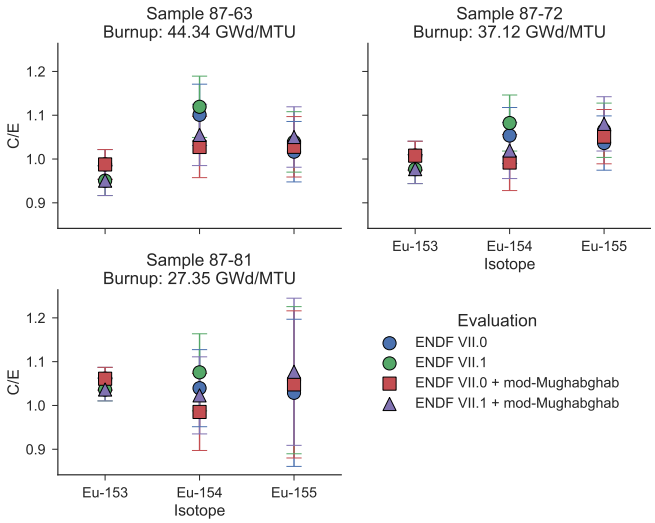

Fig. 12. C/E values for ^{153}Eu, ^{154}Eu, and ^{155}Eu for the Calvert Cliffs rod MKP-109 benchmark for each nuclear data evaluation considered.

Figure 12 shows the evaluated benchmarks for ^{153}Eu, ^{154}Eu, and ^{155}Eu for the three Calvert Cliffs samples from rod MKP-109. Similar to the TMI-1 samples, one observed improved agreement with experimental benchmark values using the corrected ^{154}Eu evaluation of about 6–6.3%, placing each sample evaluation well within the 2-σ uncertainty bounds; this is summarized as Table V. As before, the ENDF/B-VII.1 evaluation exhibits slightly higher ^{154}Eu inventories; likewise, the ^{154}Eu data correction introduces nominally higher (1–1.5%) inventories of ^{155}Eu.

Figure 13 illustrates the trends in Eu isotopes for the

TABLE IV. C/E values for ^{154}Eu for all evaluated samples and each nuclear data evaluation for TMI-1 assembly NJ05YU.

Sample	$\sigma_{meas.}$	C/E			
		ENDF VII.0	ENDF VII.1	ENDF VII.0 + mod-Mughabghab	ENDF VII.1 + mod-Mughabghab
AG536-C2D1	0.0220	1.1048	1.1193	1.0384	1.0550
AG536-C2D2	0.0200	1.1242	1.1388	1.0574	1.0731
AG616-A1	0.0200	1.1281	1.1497	1.0629	1.0860
AG616-B1	0.0200	1.1486	1.1622	1.0769	1.0936
AG616-B2	0.0210	1.0700	1.0855	1.0048	1.0221
Average		1.1151	1.1311	1.0481	1.0660

TABLE V. C/E values for ^{154}Eu for all evaluated samples and each nuclear data evaluation for Calvert Cliffs rod MKP-109.

Sample	$\sigma_{meas.}$	C/E			
		ENDF VII.0	ENDF VII.1	ENDF VII.0 + mod-Mughabghab	ENDF VII.1 + mod-Mughabghab
87-81	0.0880	1.0395	1.0757	0.9852	1.0230
87-72	0.0640	1.0537	1.0822	0.9920	1.0194
87-63	0.0700	1.1009	1.1193	1.0275	1.0550
Average		1.0647	1.0924	1.0016	1.0325

Vandellós-II rod WZR0058 samples. Here again one observes a consistently improved agreement for ^{154}Eu across all samples using the modified ^{154}Eu thermal-region evaluation, with average improvements of 4.5 and 6.3% for ENDF/B-VII.0 and VII.1, respectively; these results are summarized as Table VI.

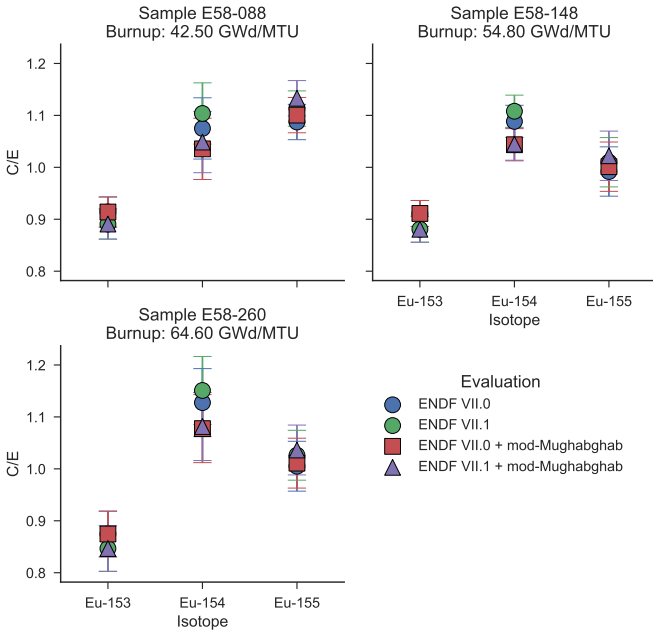

Fig. 13. C/E values for ^{153}Eu, ^{154}Eu, and ^{155}Eu for the Vandellós-II WZR0058 assembly benchmark for each nuclear data evaluation considered.

Notably, the change to ^{155}Eu inventories for the Vandellós samples resulting from the correction to the ^{154}Eu is remarkably small (generally on the order of 1% or less), potentially owing to the relatively high burnup of these samples (thereby cancelling out the effect on ^{155}Eu via increased capture rates).

In Figure 14, the benchmark results for each nuclear data evaluation is presented for the REBUS GKN-II sample. For this sample, the decrease in the over-prediction of ^{154}Eu is consistent with prior samples, showing a decreased prediction of ^{154}Eu of about 6.5% (as seen in Table VII, a significant improvement.

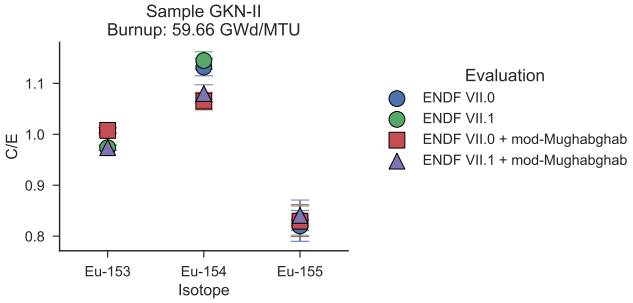

Fig. 14. C/E values for ^{153}Eu, ^{154}Eu, and ^{155}Eu for the REBUS GKN-II benchmark for each nuclear data evaluation considered.

Figure 15 illustrates the benchmarks for europium isotopes performed for the ARIANE GU1 sample. The improvement in the ^{154}Eu predictions using the corrected evaluation are slightly greater than other samples at about 7.6-7.7% for ENDF/B-VII.0 and VII.1, respectively (as indicated in Table VII). A notable feature of the GU1 sample is its proximity to a water hole in the assembly evaluated in the ARIANE

TABLE VI. C/E values for ^{154}Eu for all evaluated samples and each nuclear data evaluation for Vandellós-II rod WZR0058.

Sample	$\sigma_{meas.}$	C/E			
		ENDF VII.0	ENDF VII.1	ENDF VII.0 + mod-Mughabghab	ENDF VII.1 + mod-Mughabghab
E58-088	0.0590	1.0749	1.1037	1.0355	1.0487
E58-148	0.0310	1.0885	1.1080	1.0435	1.0447
E58-260	0.0655	1.1275	1.1509	1.0775	1.0815
Average		1.0970	1.1209	1.0522	1.0583

TABLE VII. C/E values for ^{154}Eu for each nuclear data evaluation for the REBUS GKN-II and ARIANE GU1 samples.

Sample	$\sigma_{meas.}$	C/E			
		ENDF VII.0	ENDF VII.1	ENDF VII.0 + mod-Mughabghab	ENDF VII.1 + mod-Mughabghab
REBUS GKN-II	0.0172	1.1320	1.1448	1.0652	1.0800
ARIANE GU1	0.0195	1.1283	1.1391	1.0509	1.0630

benchmark; this would imply a softer spectrum in this region (and therefore, a greater sensitivity to the thermal-region behavior of the ^{154}Eu capture cross-section). This hypothesis is further borne out in analysis of the Pickering-A CANDU PHWR sample, which shows both the greatest overestimation of ^{154}Eu as well as the largest difference in the overestimation resulting from the corrected evaluation.

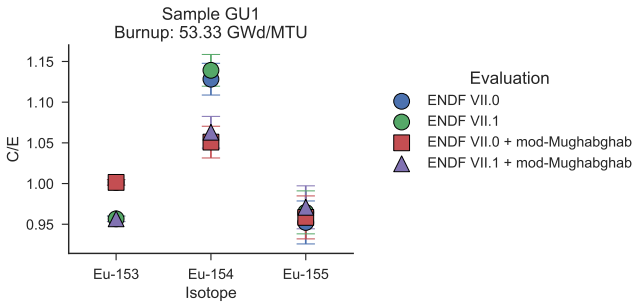

Fig. 15. C/E values for ^{153}Eu, ^{154}Eu, and ^{155}Eu for the ARIANE benchmark for each nuclear data evaluation considered.

Finally, Figure 16 shows the benchmarks for ^{154}Eu and ^{155}Eu for the Pickering-A CANDU 28-element bundle sample. Here, the change between nuclear data evaluations is most extreme of all samples, owing to the highly thermalized spectrum of the CANDU assembly; i.e., because of the higher relative thermal neutron population in the deuterium-moderated core, effects in the thermal region of the cross-section are expected to be comparatively more pronounced, as is observed here, with a 6.9% and 8.4% change for the corrections to ENDF/B-VII.0 and VII.1, respectively (illustrated in Table VIII.

In general, one will observe that while the corrected evaluation for the CANDU PHWR sample again produces substantially improved agreement with the experimental benchmark, the calculated values still lie well outside of the 2-σ bounds for the corrected ENDF/B-VII.1 evaluation, implying that

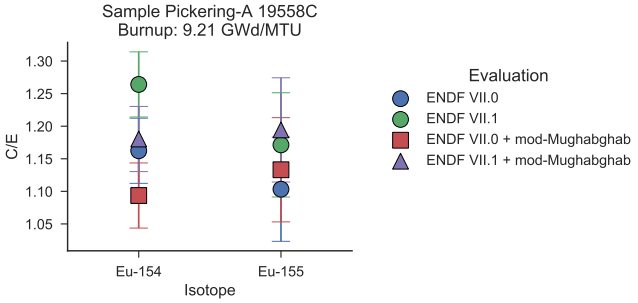

Fig. 16. C/E values for ^{154}Eu and ^{155}Eu for the Pickering-A CANDU 28-element assembly benchmark for each nuclear data evaluation considered.

the proposed correction may yet still underestimate the true thermal-region capture cross-section.

2. Analysis of trends in ^{154}Eu as a function of sample burnup

A comparison of the ^{154}Eu inventories for PWR benchmarks is illustrated as a function of burnup in Figure 17. Here, several trends are apparent: first, that the over-prediction in ^{154}Eu inventories exhibits a linear relationship to the sample burnup, with higher burnups showing a higher over-prediction in ^{154}Eu inventories. This behavior would be consistent with an underestimation in the capture cross-section (i.e., the underestimation in ^{154}Eu capture reactions grows with cumulative exposure).

While the modified ENDF/B-VII.1 evaluation shows a slightly higher C/E value compared to VII.0 (due to the modification of the ^{153}Eu thermal capture cross-section / production rate of ^{154}Eu), in general the modifications based on Mughabghab produce a significantly improved agreement to experimental data, on the order of 5–8% across all samples.

Furthermore, the corrected evaluations for ENDF/B-VII.0

TABLE VIII. C/E values for ^{154}Eu for each nuclear data evaluation for the Pickering-A 19558C CANDU 28-element sample.

Sample	$\sigma_{meas.}$	C/E			
		ENDF VII.0	ENDF VII.1	ENDF VII.0 + mod-Mughabghab	ENDF VII.1 + mod-Mughabghab
Pickering-A 19558C	0.0500	1.1623	1.2641	1.0936	1.1803

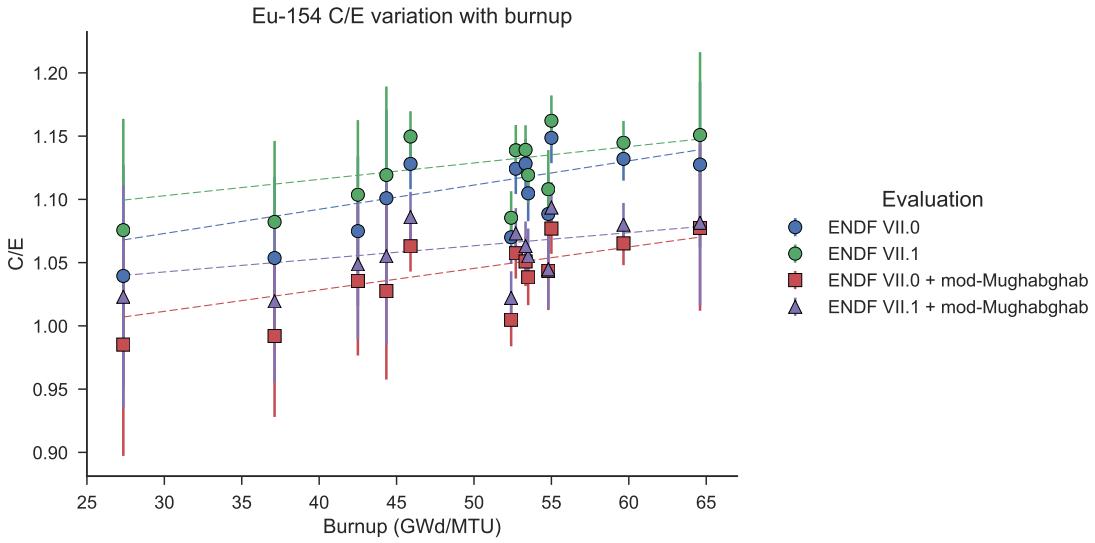

Fig. 17. C/E values for ^{154}Eu for all PWR-based fuel benchmarks and evaluations considered (i.e., all benchmarks save for the CANDU 28-element assembly), evaluated as a function of sample burnup. One will observe that discrepancies in the predicted ^{154}Eu follow a linear trend with burnup, especially for the original ENDF/B-VII.0 and VII.1 evaluations.

and VII.1 show a decreased slope for the correlation of the bias in ^{154}Eu inventories and burnup compared to the present evaluations, implying that the corrected evaluation mitigates some of the biases introduced as a function of burnup.

IV. CONCLUSIONS

Based on the series of integral spent fuel benchmarks presented within this study, there exists compelling evidence for an under-estimation of the ^{154}Eu thermal radiative capture cross-section in the ENDF/B-VII.0 and VII.1 evaluations, leading to a consistently observed bias in calculated ^{154}Eu inventories. In particular, a wide range of spent fuel benchmarks representing a diverse series of PWR lattice types and final discharge burnups show consistent biases in the predictions of ^{154}Eu using modern nuclear data, ranging from 7.5–15%. Proposed modifications to the thermal capture cross-section, such as an adjustment of the first resolved resonance to 0.188 eV (and proportional adjustment ot the neutron width) largely appear to correct this overestimation by approximately 6–8%, although some residual over-estimation of ^{154}Eu remains, particularly for samples with highly thermalized spectra such as CANDU PHWR assemblies.

From this study, a subsequent re-evaluation (potentially including new irradiation experiments) of the ^{154}Eu capture cross-section would appear to be warranted in order to both confirm and help to refine future evaluations. In particular, given the importance of ^{154}Eu for spent fuel burnup measurement, the existence of a systematic bias in the nuclear data could have potentially significant deleterious consequences for the development and validation of passive gamma-based spent fuel measurement and assay systems. Further, over-estimations in the ^{154}Eu will lead to moderate unnecessary conservatism for dry cask storage dose and shielding evaluations. In as much, a corrected evaluation would offer broad benefit to multiple nuclear data user communities.

V. ACKNOWLEDGMENTS

This work was supported by an Nuclear Energy University Programs (NEUP) grant sponsored by the U.S. Department of Energy, Office of Nuclear Energy, award number DE-NE0000737. The author also wishes to acknowledge the contributions of Nathan Shoman, who began the work on the TMI-1 lattice used in this study; he also wishes to express his sincere appreciation to Shane Hart, Doro Wiarda, and Mark Williams of Oak Ridge National Laboratory for their invaluable assistance in preparing modified AMPX master libraries for testing the ^{154}Eu thermal capture cross-sections.

REFERENCES

1. J. R. PHILLIPS, "Irradiated Fuel Measurements," in "Passive Nondestructive Analysis of Nuclear Materials," Los Alamos National Laboratory, Los Alamos, NM (March 1991).
2. A. LEBRUN and G. BIGNAN, "Nondestructive Assay of Nuclear Low-Enriched Uranium Spent Fuels for Burnup Credit Application," *Nuclear Technology*, **135**, *3*, 216–229 (September 2001).
3. C. WILLMAN, A. HÅKANSSON, O. OSIFO, A. BÄCKLIN, and S. J. SVÄRD, "Nondestructive assay of spent nuclear fuel with gamma-ray spectroscopy," *Annals of Nuclear Energy*, **33**, *5*, 427–438 (2006).
4. A. FAVALLI, D. VO, B. GROGAN, P. JANSSON, H. LILJENFELDT, V. MOZIN, P. SCHWALBACH, A. SJÖLAND, S. J. TOBIN, H. TRELLUE, and S. VACCARO, "Determining initial enrichment, burnup, and cooling time of pressurized-water-reactor spent fuel assemblies by analyzing passive gamma spectra measured at the Clab interim-fuel storage facility in Sweden," *Nuclear Instruments and Methods in Physics Research Section A: Accelerators, Spectrometers, Detectors and Associated Equipment*, **820**, 102 – 111 (2016).
5. S. E. SKUTNIK, "Proposed re-evaluation of the ^{154}Eu thermal (n,γ) capture cross-section based on spent fuel benchmarking studies," *Annals of Nuclear Energy*, **99**, 80 – 107 (2017).
6. I. C. GAULD, J. M. GIAQUINTO, J. S. DELASHMITT, J. HU, G. ILAS, T. J. HAVERLOCK, and C. ROMANO, "Re-evaluation of spent nuclear fuel assay data for the Three Mile Island unit 1 reactor and application to code validation," *Annals of Nuclear Energy*, **87, Part 2**, 267 – 281 (2016).
7. G. ILAS, I. C. GAULD, F. C. DIFILIPPO, and M. EMMETT, "Analysis of Experimental Data for High Burnup PWR Spent Fuel Isotopic Validation–Calvert Cliffs, Takahama, and Three Mile Island Reactors," Tech. Rep. NUREG/CR-6968 / ORNL/TM-2008/071, U.S. Nuclear Regulatory Commission (NRC) (February 2010).
8. G. ILAS, I. C. GAULD, and B. D. MURPHY, "Analysis of Experimental Data for High Burnup PWR Spent Fuel Isotopic Validation–ARIANE and REBUS Programs (UO_2 Fuel)," Tech. Rep. NUREG/CR-6969 / ORNL/TM-2008/072, U.S. Nuclear Regulatory Commission (NRC) (February 2010).
9. G. ILAS and I. C. GAULD, "Analysis of Experimental Data for High-Burnup PWR Spent Fuel Isotopic Validation–Vandellós II Reactor," Tech. Rep. NUREG/CR-7013 / ORNL/TM-2009/321, U.S. Nuclear Regulatory Commission (NRC) (January 2011).
10. N. T. SHOMAN and S. E. SKUTNIK, "Development of modern CANDU PHWR cross-section libraries for SCALE," *Nuclear Engineering and Design*, **302, Part A**, 56 – 67 (2016).
11. T. SEKINE, S.-I. ICHIKAWA, and S. BABA, "Triple Neutron Capture of ^{153}Eu in a Reactor: The Cross Sections of ^{154}Eu and ^{155}Eu," *International Journal of Radiation Applications and Instrumentation. Part A. Applied Radiation and Isotopes*, **38**, *7*, 513–516 (1987).
12. S. F. MUGHABGHAB, *Atlas of Neutron Resonances, Fifth Edition: Resonance Parameters and Thermal Cross Sections. Z=1–100*, Elsevier Science (April 2006).
13. M. CHADWICK ET AL., "ENDF/B-VII.0: Next Generation Evaluated Nuclear Data Library for Nuclear Science and Technology," *Nuclear Data Sheets*, **107**, *12*, 2931–3060 (December 2006), Evaluated Nuclear Data File ENDF/B-VII.0.
14. CROSS-SECTION EVALUATION WORKING GROUP, "ENDF/B-VI Summary Documentation," Tech. Rep. BNL-NCS-17541 (ENDF-201), Brookhaven National Laboratory (1998), Data Library ENDF/B-VI, update 1998, by the U.S. National Nuclear Data Center on behalf of the Cross-Section Evaluation Working Group.
15. R. J. HAYDEN, J. H. REYNOLDS, and M. G. INGHRAM, "Reactions Induced by Slow Neutron Irradiation of Europium," *Phys. Rev.*, **75**, 1500–1507 (May 1949).
16. V. P. VERTEBNYJ, P. N. VORONA, A. I. KAL'CHENKO, V. G. KRIVENKO, and V. A. PSHENICHNYJ, "Neutron Resonances of the Radioactive Nuclides Eu-154 and Eu-155," *Vop. At.Nauki i Tekhn., Ser.Yadernye Konstanty*, **5**, *49*, 16 (1982).
17. V. A. ANUFRIEV, S. I. BABICH, A. G. KOLESOV, V. N. NEFELOV, V. A. PORUCHIKOV, V. A. SAFONOV, A. P. CHETVERIKOV, V. S. ARTAMONOV, R. N. IVANOV, and S. M. KALEBIN, "Measurement of the total neutron cross sections of ^{153}Eu, ^{154}Eu, and ^{155}Eu," *Soviet Atomic Energy*, **46**, *3*, 182–185 (1979).
18. G. RADULESCU, I. C. GAULD, and G. ILAS, "SCALE 5.1 Predictions of PWR Spent Nuclear Fuel Isotopic Compositions," Tech. Rep. ORNL/TM-2010/44, Oak Ridge National Laboratory (March 2010).
19. O. W. HERMANN, S. M. BOWMAN, M. C. BRADY, and C. V. PARKS, "Validation of the SCALE System for PWR Spent Fuel Isotopic Composition Analyses," Tech. Rep. ORNL/TM-12667, Oak Ridge National Laboratory (March 1995).
20. K. SUYAMA and H. MOCHIZUKI, "Corrections to the ^{148}Nd method of evaluation of burnup for the PIE samples from Mihama-3 and Genkai-1 reactors," *Annals of Nuclear Energy*, **33**, 335–352 (2006).
21. I. C. GAULD and K. A. LITWIN, "Verification and Validation of the ORIGEN-S Code and Nuclear Data Libraries," Tech. Rep. RC-1429 / COG-I-95-150, Atomic Energy of Canada Limited (AECL) (August 1995).
22. J. TAIT, I. GAULD, and A. H. KERR, "Validation of the ORIGEN-S Code for Predicting Radionuclide Inventories in Used CANDU Fuel," *Journal of Nuclear Materials*, **223**, *2*, 109–121 (May 1995).
23. I. C. GAULD, P. CARLSON, and K. LITWIN, "Production and Validation of ORIGEN-S Cross-Section Libraries for CANDU Reactor Fuel Studies," Tech. Rep. RC-1442; COG-I-95-200, Whiteshell Laboratories (October 1995).